Neural control of the healthy pectoralis major from low-to-moderate isometric contractions

Tea Lulic-Kuryllo[1], Christopher K. Thompson[2], Ning Jiang[3], Francesco Negro[4*], Clark R. Dickerson[1]

[1]Department of Kinesiology, University of Waterloo, Waterloo, Canada
[2]Department of Health and Rehabilitation Sciences, Temple University, Philadelphia, USA
[3]Department of Systems Design Engineering, University of Waterloo, Waterloo, Canada
[4]Department of Clinical and Experimental Sciences, Università degli Studi di Brescia, Brescia, Italy

Submission to *Journal of Neurophysiology*

Abstract: 215/250 words

New and Noteworthy: 71/75 words

Figures: 6

Tables: 3

Running head: Neural control of pectoralis major

*Corresponding author:
Department of Clinical and Experimental Sciences
Università degli Studi di Brescia
Viale Europa 11
25123 Brescia, Italy
E-mail: francesco.negro@unibs.it
Phone: +39 0303717452
Fax: +39 0303717443

Conflicts of interest/Competing interests

The authors report no conflicts of interest.

Link to original article in APS: https://journals.physiology.org/doi/abs/10.1152/jn.00046.2021

Abstract (215/250 words)

The pectoralis major critically enables arm movement in several directions. However, its neural control remains unknown. High-density electromyography (HD-sEMG) was acquired from the pectoralis major in two sets of experiments in healthy young adults. Participants performed ramp-and-hold isometric contractions in: adduction, internal rotation, flexion, and horizontal adduction at three force levels: 15%, 25%, and 50% scaled to task-specific maximal voluntary force (MVF). HD-sEMG signals were decomposed into motor unit spike trains using a convolutive blind source separation algorithm and matched across force levels using a motor unit matching algorithm. The mean discharge rate and coefficient of variation were quantified across the hold and compared between 15% and 25% MVF across all tasks, while comparisons between 25 and 50% MVF were made where available. Mean motor unit discharge rate was not significantly different between 15% and 25% MVF (all $p > 0.05$) across all tasks or between 25% and 50% MVF in horizontal adduction ($p = 0.11$), indicating an apparent saturation across force levels and the absence of rate coding. These findings suggest that the pectoralis major likely relies on motor unit recruitment to increase force, providing first-line evidence of motor unit recruitment in this muscle and paving the way for more deliberate investigations of the pectoralis major involvement in shoulder function.

NEW AND NOTEWORTHY (71/75 words)

This work is the first to investigate the relative contribution of rate coding and motor unit recruitment in the pectoralis major muscle in several functionally relevant tasks and across varying force levels in healthy adults. Our results demonstrate the absence of motor unit rate coding with an increase in EMG amplitude with increases in force level in all tasks examined, indicating that the pectoralis major relies on motor unit recruitment to increase force.

Keywords: motor unit; motor unit decomposition; motor unit recruitment; shoulder

INTRODUCTION

The pectoralis major has a multifunctional role in humeral mobility, assisting in humeral adduction, flexion, internal rotation, and extension against resistance (Ackland et al. 2008; Ackland and Pandy, 2011; Brown et al. 2007; Leonardis et al. 2017; Lulic-Kuryllo et al. 2021; Paton and Brown, 1994; Wickham et al. 2004; Wickham et al. 2012; Wolfe et al. 1992). Several studies using surface electromyography (sEMG) have attempted to infer the neural and neuromuscular control of this muscle using normalized EMG amplitudes (Paton and Brown, 1994; Wickham et al. 2012). However, the EMG amplitude is affected by several physiological and non-physiological factors and reflects both central and peripheral motor unit properties (Farina et al. 2004; Martinez-Valdes et al. 2018). A single study documented the pectoralis major's motor unit discharge rate at maximal contractions in a single isometric task (Bracchi et al. 1966). However, the pectoralis major has a considerable role across several upper extremity movements and activates across varying force levels. As such, the exact mechanisms behind pectoralis major force modulation and, therefore, the relative role of motor unit recruitment and rate coding across several functionally relevant tasks and varying force levels in this muscle remain unknown.

Previous studies have documented divergent neural control of distal and more proximal arm muscles in force generation. For example, using intramuscular electromyography, deltoid was shown to predominantly rely on motor unit recruitment with increasing force level, changing the motor unit firing rate only ~3.4 pps between 40% and 80% MVC (De Luca et al. 1982). Similarly, the biceps brachii, upper trapezius, and brachialis were observed to rely predominantly on motor unit recruitment (De Luca et al. 1982; De Luca, 1985; Kanosue et al. 1979; Kukulka et al. 1981; Seki et al. 1996; Westgaard and De Luca, 2001). In contrast, more distal muscles, such as the first dorsal interosseus, the adductor pollicis and extensor digitorum communis, predominantly rely on rate coding (De Luca et al. 1982; Kukulka et al. 1981; Milner-Brown et al. 1973; Monster and Chan, 1977; Seki et al. 1996; Westgaard and De Luca, 2001). These findings indicate that larger, more proximal shoulder muscles may predominantly rely on motor unit recruitment in force generation.

Since the pectoralis major is a large, proximal muscle of the shoulder complex, the logical expectation is that this muscle would rely on motor unit recruitment to generate force. However, motor unit recruitment is challenging to assess methodologically, as this would require recording from a representative motor unit pool across several force levels. Alternatively, the relative role of motor unit recruitment can be determined by examining the rate coding and the EMG amplitude across force levels. Specifically, the lack of rate coding and a significant increase in the EMG amplitude with change in force level may be used to indicate that motor unit recruitment is a predominant control strategy. Therefore, the purpose of this work was to investigate the neural control of the pectoralis major in healthy, young adults across several tasks at varying force levels. We hypothesized that the pectoralis major would rely on motor unit recruitment for increases in force.

METHODS

Participants

This work consisted of two linked experiments, which examined pectoralis major activation in six functionally relevant tasks. In Experiment 1, eighteen and twenty healthy, right-hand dominant males and females, respectively, participated (Males: 25 ± 4.7 years; Females: 22.4 ± 2.2 years). In Experiment 2, ten and nine healthy, right-hand dominant males and females participated (Males: 25.8 ± 5.3 years; Females: 24.5 ± 3.1 years). All participants were free from musculoskeletal or neurological injuries and low back pain in the past six months and were recreationally active. No participants tested positive for impingement signs, as determined by the Hawkin's impingement and the Apley's Scratch test. Participants were instructed by the investigator not to consume any caffeinated drinks the morning of the session due to the possible effects of caffeine on the motoneuron firing rates (Walton et al. 2002) and to refrain from engaging in strenuous physical activity for 24 hours before the session. Females wore a regular bra (i.e., no sports bra) to mitigate the high-density surface EMG (HD-sEMG) array compression during the experimental protocol. This study was reviewed and received ethics clearance from the Institutional Office of Research Ethics (ORE #31747 and ORE #40849) and conformed to the Declaration of Helsinki.

High-density surface electromyography

Two 64-channel HD-sEMG arrays acquired pectoralis major activation in monopolar mode (ELSCH064NM3, SpesMedica, Battipaglia, Italy; **Figure 1A**). Electrode arrays consisted of channels in an 8x8 matrix with a 10 mm inter-electrode distance. Before applying the arrays, the skin overlying the pectoralis major was shaved (in males) and cleaned with abrasive paste and water (Piervirgili et al. 2014). The electrode arrays were applied on the skin using a 1 mm thick two-sided adhesive foam. The holes were filled with the electroconductive gel. The superior array was placed ~ 2 cm inferior to the clavicle. The middle of the superior array was positioned between the sternum and the axilla and parallel to the muscle fibers. The inferior array was placed directly below the superior array. The arrays were fixed with adhesive tape and connected to the 128 channel EMG amplifier (EMGUSB2+, OTBioelecttronica, Torino, Italy). One wet reference band was wrapped around the participant's right wrist, while a reference electrode was placed on the right clavicle. All HD-sEMG signals were bandpass filtered with a cut-off frequency between 10 – 500 Hz and sampled at 2048 Hz with a 12-bit A/D converter (5V dynamic range). HD-sEMG signals were amplified by a factor between 100-5000 V/V. The channel saturation was monitored online in the OTBiolab software (OTBiolab, OTBioelecttronica, Torino, Italy).

Force acquisition

The raw voltage was acquired during submaximal and maximal trials concurrently with HD-sEMG. The force was exerted against a custom-built arm cuff attached to a six-degree-of-freedom force transducer (MC3A, AMTI MA, USA) mounted on a robotic arm (**Figure 2A** and **2B**; Motoman Robotics Division, Yaskawa America, USA). The arm cuff was located either in the middle of the upper arm or forearm. The arm was secured in the arm-cuff by padding to mitigate any arm movement during the submaximal and maximal trial performance. Force at the upper arm or forearm (depending on the task) was sampled at 1500 Hz and amplified (1000x) using VICON Nexus 1.7.1 software.

Experimental protocol

The experimental protocol included the performance of several maximal voluntary force trials (MVF) and isometric ramp and hold submaximal trials in five tasks at three force levels. The participant sat on a chair with the trunk secured with a padded strap during all procedures. All participants underwent a brief warm-up that included training on how to generate a maximal contraction of the pectoralis major in different tasks and practicing force exertions against an arm-cuff with visual feedback of the force provided on a monitor. The warm-up and training served to precondition the muscle-tendon unit (Maganaris et al. 2002) and familiarize the participant with the task. Further, participants were told to practice following the trapezoid as closely as possible.

Following training and familiarization, participants performed two trials of task-specific, five-second MVFs against an arm cuff. Maximal and submaximal trials were performed in the following tasks (**Figures 2B** and **2C**): Experiment 1: a) adduction at 60° of humeral elevation, 0° of plane of elevation and axial rotation; b) internal rotation at 60° of humeral elevation, 0° of plane of elevation and axial rotation; c) adduction at 90° of humeral elevation, 0° of plane of elevation and axial rotation; and d) adduction at 90° of humeral elevation and axial rotation and 0° of plane of elevation; and Experiment 2: a) flexion at 20° of humeral elevation, 0° of plane of elevation and axial rotation and b) horizontal adduction at 90° of humeral elevation and 50° of plane of elevation. These tasks were chosen because they typically require pectoralis major to act as a prime mover, synergist, or an antagonist (Ackland et al. 2008; Ackland and Pandy, 2011; Paton and Brown, 1992; Wickham et al. 2012; Wolfe et al. 1992). During MVF performance, participants were verbally encouraged by the investigators. Each MVF was separated by ~2 minutes of rest. MVFs were quantified using a custom-made program in LabVIEW (National Instruments). During the MVF performance, off-axis forces were monitored in the LabVIEW program, such that participants were required to achieve above 80% of the total force along the intended transducer axis. The mean force of two task-specific MVFs was used to scale all analogous submaximal trials.

For each task, participants performed submaximal ramp and hold isometric trials scaled to the task-specific MVF. The force levels included: 15%, 25%, and 50% MVF (**Figure 1B**). Participants performed each force level twice, and trials lasted 60 seconds for 15% and 25% MVF and 30 seconds for 50% MVF with three to five-minute rest breaks between the trials.

Each submaximal trial consisted of a ramp up/down and hold. For 15% and 25% MVF, participants ramped up and down ~2% MVF/s and at 50% MVF, ~3% MVF/s. Tasks were block randomized within a participant. Force levels were randomized within each task, with each submaximal trial performed consecutively. Visual feedback was provided on a monitor ~1 meter from the participant as a white trapezoid on a black screen and displayed the required submaximal force level. Live feedback of the exerted force against the arm cuff was provided as a pink line overlaying the trapezoid. The investigators monitored the submaximal task performance, and if the participant's live feedback deviated more than ~5% from the trapezoid, the trial acquisition was stopped, the participant was reminded to follow the trapezoid as closely as possible, and the trial was repeated. However, this did not frequently occur as the familiarization, and the training part of the experiment mitigated such occurrences.

Electrocardiography

Electrocardiography (ECG) was also acquired concurrently with HD-sEMG and force. The ECG was collected to eliminate the heart rate artefact from HD-sEMG amplitude measures in post-processing steps. Three silver-silver chloride (Ag-AgCl) disposable electrodes were used to acquire ECG in monopolar mode and were placed over the left chest at the 6^{th} coastal level, approximately along the anterior axillary line, and medially at the sternocostalis junction. Before the placement of the electrodes, the area was shaved if necessary, cleaned with abrasive gel and water. ECG was acquired using a wireless telemetry system (Noraxon Telemyo 2400 T G2 Noraxon, Arizona, USA). ECG signal was filtered with a bandpass from 10-1000 Hz and differentially amplified with a CMRR > 100 dB and an input impedance of 100 MΩ. Analog signals were converted to digital using a 16-bit A/D card with a ±10 V range, and sampling frequency was set to 1500 Hz.

Data Analysis

Force

Raw voltage acquired by the force transducer in submaximal and maximal trials was further processed. Raw voltage in X, Y, and Z directions was filtered using a 3rd order low-pass Butterworth filter with a cut-off frequency of 15 Hz and converted to Newtons using a custom-made program in MATLAB. For maximal trials, the mean of 3-second data surrounding the maximal force achieved was extracted. The force acquired in the intended direction during submaximal trials was then normalized to the mean of the two maximal values quantified during the task-specific MVFs. Normalized force data was used to confirm that all participants exerted similar force levels at 15%, 25%, or 50% MVF.

EMG amplitude

Quantification of mean HD-sEMG amplitude involved the removal of the ECG artifact and normalization of data. ECG was removed from monopolar HD-sEMG signals. ECG was first interpolated to 2048 Hz to match the sampling frequency of the HD-sEMG and then cross-correlated with the HD-sEMG signals to match each ECG peak's timing. Each channel and trial were visually inspected to confirm that the algorithm correctly matched the ECG peaks. The precise timing of each ECG peak was determined, and the frames corresponding to the ECG peaks were removed from the quantification of the root mean square (RMS) amplitude. The ECG was only removed from the RMS amplitude quantification and was not performed for the decomposition stage (described below). Following this, a differential derivation for the superior array was quantified from the axilla towards the sternum, reducing the number of channels to 56. The force was used as a reference to localize the hold on the trapezoid. The most stable part of the resultant force was selected by dividing the force signal into five-second segments and performing the analyses on the one with the lowest coefficient of variation in the first half of the sustained hold. All submaximal data were normalized to channel-specific maxima. The mean of all channels was then quantified to determine the mean EMG amplitude.

HD-sEMG decomposition

HD-sEMG processing involved several steps. Before decomposition, each HD-sEMG channel was visually inspected in a custom-made program in MATLAB. Any channels that were saturated, had an artifact, or had insufficient skin contact (i.e., no signal detected) were removed from further analyses. Before decomposition, monopolar HD-sEMG recordings were bandpass filtered with a 3rd order Butterworth filter between 20-500 Hz. We did not remove the ECG artefact prior to data decomposition, as the ECG is out of the range of motor unit instantaneous discharge rates and the decomposition algorithm identifies it as a source. HD-sEMG signals were decomposed using convolutive blind source separation previously validated in a broad range of forces in several muscles (Martinez-Valdes et al. 2018; Negro et al. 2016; Perreira et al. 2019; Thompson et al. 2018). An experienced investigator visually inspected and manually edited all decomposed motor units as previously performed in several studies (see for example Afsharipour et al. 2020; Cogliati et al. 2020; Boccia et al. 2019). Specifically, all decomposition results were visually inspected, and the same investigator manually identified and removed lower quality motor unit spikes from the calculation of the separation filter. After excluding poor quality motor unit spike-train intervals, the motor unit filter was re-calculated and re-applied to the entire EMG signal, which allowed for an objective re-estimation of the entire motor unit spike train (Del Vecchio et al. 2020). This manual analysis allowed us to retain only those motor units that were characterized by high accuracy. The accuracy of the decomposition was determined using the silhouette measure (SIL), which is a normalized accuracy index for EMG decomposition, detailed in (Negro et al. 2016). Only those motor units with a reliable discharge pattern and SIL > 0.9 were included in subsequent analyses.

Motor unit matching, discharge rate, and coefficient of variation

In male participants, a modified and simplified version of the motor unit tracking algorithm to that of previous studies was used to match the motor units between different force levels within the same task (**Figure 1C**; Martinez-Valdes et al. 2017; Martinez-Valdes et al. 2017; Del Vecchio et al. 2020). This tracking algorithm uses cross-correlation analyses between two-dimensional motor unit action potentials, extracted using spike-triggered averaging from the HD-sEMG signals at the discharge times of the motor units identified by the blind convolutive source separation (Martinez-Valdes et al. 2017). Each motor unit match was visually inspected. Only motor units with motor unit action potential waveforms correlated by > 0.8 at the end with respect to the beginning of the two force levels were included in further analyses. The mean discharge rate and coefficient of variation (CoV) of the inter-spike interval were quantified for 5-second intervals across the sustained hold for the matched motor units. Our analyses focused on the sustained part of the trapezoid. The discharge rate was quantified from the mean values of the inverse of the interspike interval. CoV of the inter-spike interval was quantified as the standard deviation of the inter-spike interval divided by the mean inter-spike interval.

Motor unit analyses in females focused on the unmatched motor unit data decomposed from the superior array due to the breast tissue overlying the lower sternocostal regions. The focus was placed on the unmatched motor units due to the low motor unit yield and inability to match many motor units across force levels. The mean discharge rate and CoV of inter-spike-interval were quantified for the unmatched motor units. Motor unit tracking was implemented to determine if this method is feasible in successfully decomposed motor units.

Technical issues and data removal

Some technical issues arose during the collection of the HD-sEMG data. Due to the technical issues with the force feedback at 25% MVF in flexion, one male participant's data was removed from the motor unit and EMG amplitude analyses in this task. Further, technical issues existed in maximal trials for the horizontal adduction in one male participant, preventing the normalization of EMG amplitude data and resulting in the removal of this participant's data from EMG amplitude analyses. Adduction from 90° elevation and axial rotation (ADER) did not yield any motor units in males, and therefore, this task was not included in motor unit analyses. Decomposition in male participants was also not successful for 50% MVF in any tasks, except in horizontal adduction. Lastly, decomposition in females was not successful in flexion, horizontal adduction, and adduction 60.

Statistical Analyses

All statistical analyses were performed using SPSS (IBM, version 21). Before statistical comparisons, the data were checked for normality using the Shapiro-Wilks test. Not normally distributed data were log-transformed. Statistical analyses were performed for each task separately because the arm position was different between the tasks. Moreover, the statistical analyses focused only on the matched motor units in males. Specifically, the low motor unit yield in females and inability to match motor units between force levels prevented from the ability to perform statistical analyses on female data. For mean EMG amplitude, a paired samples t-test was used to compare if the amplitude changed between 15% and 25% MVF within each task in adduction 60, adduction 90, internal rotation, flexion, and horizontal adduction in males. Due to the low number of participants (N = 3), statistical analyses were not performed between 25% and 50% MVF in horizontal adduction. A paired-samples t-test was used to compare if the mean discharge rate and CoV differed between 15% and 25% MVF within each task. For horizontal adduction, a paired samples t-test with a Bonferonni correction was used to compare the discharge rate and CoV between 15% and 25% MVF or 25% and 50% MVF. Significance was set to $p < 0.05$.

RESULTS

All participants maintained the force within 4% of the target hold (**Table 1**). In Experiment 2, MVF for each task was similar at the beginning and end of the experiment. In males, the total number of motor units decomposed across five tasks was 251 at 15% MVF and 173 at 25% MVF. A motor unit matching algorithm tracked the same motor unit across different force levels within a task. Analyses focused only on matched motor units within a task, as the arm position was not the same across tasks. Total matched motor units across force levels and tasks were 100 (see **Table 2**). Further, in horizontal adduction, 23 motor units that were successfully decomposed at 50% MVF in four male participants were matched to motor units at 25% MVF. A summary of the number of motor units decomposed in each task and force level, average values for mean normalized EMG amplitude, mean discharge rate and mean coefficient of variation of the inter-spike interval are presented in **Table 2**. Due to the challenges in decomposing HD-sEMG signals in females and a low motor unit yield, sex-related differences could not be examined, and therefore, the data were analyzed separately.

Males

Within each task, the mean normalized EMG amplitude was compared between force levels. As the force level increased, the mean normalized EMG amplitudes increased in all tasks examined (**Table 2**). In contrast, the mean discharge rate did not change despite increases in the force level in any task (**Table 2**). Within each task, no change in the instantaneous discharge rate occurred in any motor units (**Figures 3**, **4**, and **5**), despite an increase in the force level and EMG amplitude. Similarly, in a single task where we successfully decomposed motor units at 50% MVF, there was no change in the instantaneous discharge rate (**Figure 5B**), despite increased force level and EMG amplitude. Moreover, all motor units decomposed discharged on average between 12-15 pps. The motor units discharged on average between 12-18 pps within the first 5 seconds of the sustained hold irrespective of the task.

Females

General observations on unmatched motor units

Due to the low number of motor units decomposed in females, this section focuses on general observations in motor unit physiology (**Table 3**). The ability to match motor units between 15% and 25% MVF was explored in adduction 90 and adduction external 90, as two to three participants yielded successfully decomposed motor unit data at both force levels in these tasks (**Figure 6**). The discharge rate between 15% and 25% MVF in the matched motor units did not change (**Figure 6A** and **6D**), even though the force level increased (**Figure 6B** and **6E**). At 15% MVF, the mean discharge rate of unmatched motor units was ~9 pps in adduction 90, ~14.8 in internal rotation, and ~8.8 pps in adduction external 90 (**Table 3**). Although the ability to match motor units was possible in two females in two different tasks, the low number of motor units did not allow for statistical comparisons in motor unit discharge rate and CoV inter-spike-interval.

DISCUSSION

This is the first set of experiments to use motor unit matching and HD-sEMG decomposition to investigate the relative contribution of rate coding and motor unit recruitment in force modulation in the pectoralis major in a diverse range of motor tasks across varying force levels. We hypothesized that the pectoralis major would rely on motor unit recruitment to increase force. We tested this hypothesis by examining the rate coding and EMG amplitude across different force levels within a sustained portion of the voluntary isometric contraction. Our hypothesis was supported in males, as motor unit discharge rate did not significantly change between force levels, despite the significant increase in the EMG amplitude. The absence of rate coding with an increase in the EMG amplitude in the sustained part of the trapezoid was observed independent of the task. Further, the motor unit discharge rate in the first five seconds across the sustained portion of the trapezoid was high (between 12-15 pps) at relatively low force levels (i.e., 15% or 25% MVF) compared to the mean motor unit firing rates typically reported in more distal muscles at the same force level. Lastly, we observed a non-fatigue related decrease in the motor unit firing rate over time within all tasks irrespective of the force level. Although the motor unit yield was low in females, similar patterns were observed.

The matching of the same motor units allowed us to, for the first time, observe an absence of rate coding during the sustained portion of the hold in the motor units of the pectoralis major as the force level increased. These findings suggest that with an increasing synaptic current to the motor pool, the pectoralis major motoneurons do not increase their discharge rate. The reliance on motor unit recruitment for modulation of force contrasts with what is typically observed in more distal upper limb muscles. Hand and wrist muscles, which are important in fine motor control, were previously demonstrated to primarily rely on rate coding (De Luca et al. 1982; Kukulka et al. 1981; Milner-Brown et al. 1973; Monster and Chan, 1977; Seki et al. 1996; Westgaard and De Luca, 2001). In contrast, muscles of the shoulder complex involved in gross movements, such as the deltoid, upper trapezius, and biceps brachii, were shown to rely on motor unit recruitment across most of the force range (De Luca et al. 1982; De Luca, 1985; Kanosue et al. 1979; Kukulka et al. 1981; Seki et al. 1996; Westgaard and De Luca, 2001), although some rate coding was still observed. However, these studies used intramuscular fine wire or concentric needle electromyography, which are limited to the tacking of motor unit rate coding within a contraction and rely on a single waveform (Carroll et al. 2011), limiting the interpretation of these findings.

The absence of rate coding in the pectoralis major contrasts previous motor control theories regarding force modulation. Typically, the common synaptic drive to the motoneuron pool increases the rate coding of the active motor units and recruits new previously subthreshold motor units. Interestingly, most motor units recorded in this work had an average discharge rate between ~12-18 pps within the first five seconds of the sustained hold, irrespective of the force level. These discharge rates resembled those previously reported (~19.45 ± 2.6 pps) in maximal voluntary contractions of the pectoralis major (Bracchi et al. 1966). Although the force-frequency properties of the underlying motor units are presently unknown for the pectoralis major, it is likely that driving its motoneurons to higher rates will generate more force. However, the data in this work and that of others (Bracchi et al. 1966) did not record mean motor unit firing rates above ~20 pps. Therefore, the modulation of force in this muscle seems to rely on a more non-graded control by recruiting all motor units to discharge at near maximal firing rates irrespective of whether the contraction is low, moderate, or high. Additionally, irrespective of the task or force level, motor unit firing rates progressively decreased across time (De Luca et al. 1982), suggesting that the adaptation processes were similar between force levels. In general, the pectoralis major has a relatively low requirement for fine motor control, typically assisting in gross movements (i.e. humeral mobility and shoulder complex stability) or postural maintenance, and may prioritize the rate of force development. Therefore, the rate coding may not be critically important in the modulation of force in the pectoralis major, as the substantial recruitment of motor units may be enough to increase contractile force, as suggested for other large shoulder muscles (De Luca, 1985; De Luca et al. 1982).

Potential mechanisms limiting rate coding in the pectoralis major

The absence in rate coding with change in force level during the sustained hold may be explained by the contributions of the ionic currents intrinsic to the spinal motoneurons. Persistent inward currents (PICs) modulate motoneuron excitability through the activation of voltage-gated Na^+ and Ca^{2+} channels, which have particularly long-time constants. This provides a powerful depolarizing current to the motoneuron dendrites (Fuglevand et al. 2015; Lee and Heckman, 1998; 2000), which may amplify synaptic drive. Given this large conductance, activation of PICs may also saturate discharge, making the neuron relatively insensitive to further excitatory synaptic drive (Binder et al. 2020).

PICs are thought to be more pronounced in the proximal than distal muscles, as these muscles support tonic or postural muscle activation (Brownstone, 2006; Heckman et al. 2009; Johnson and Heckman, 2010; Powers and Heckman, 2017; Wilson et al. 2015). Pectoralis major assists in postural maintenance and therefore, it is plausible that the PICs acting on the motoneurons are high. Moreover, pectoralis major activation is functionally critical in the performance of gross movements and stabilization of several joints, which does not require a high degree of precision. As such, it was previously suggested that muscles that are functionally relevant in the performance of such tasks may benefit from high gains and large PICs (Johnson and Heckman, 2014; Powers and Heckman, 2017).

The activation and ultimate magnitude of the PIC is a result of both intrinsic (i.e. channel density and subtype) and extrinsic (i.e. increased neuromodulatory drive from the brainstem centers) factors. Elegant anatomical studies from the cat reveal motoneurons of the neck extensors have a greater number of both serotonin (5HT) and norepinephrine (NE) channels on the motoneuron (Maratta et al. 2015; Montague et al. 2013) (i.e. the distribution and the density of contacts from noradrenergic and serotonergic boutons on the dendrites of neck flexor motoneurons in the adult cat). It is likely that this increased channel density intrinsic to the spinal motoneurons will produce greater PICs in extensors as compared to the neck flexors. Such data are not available for other motor pools or in humans, but it is plausible that the motoneurons innervating the pectoralis major have a greater number of 5HT and/or NE channels as compared to the motoneurons with greater levels of rate modulation. Further, it is also possible that the descending 5HT and NE projections are greater to more proximal muscles. Motoneurons innervating axial muscles are located more midline in the spinal cord (Elliott, 1942; Vanderhorst and Holstege, 1997) and may receive greater neuromodulatory drive than the more laterally located motoneurons innervating distal musculature.

Alternatively, the inhibitory drive may have played a significant role in limiting the motor unit rate coding. Specifically, "balanced" inhibition, where the magnitude of inhibition is proportional to excitatory motor command (Berg et al. 2007) may limit motor unit rate coding (Johnson and Heckman, 2014; Powers and Heckman, 2017). Most notably, balanced inhibition is involved in the control of breathing (de Almeida and Kirkwood, 2010), which is also one of the key roles of the pectoralis major (Bolser and Reier, 1998; Lasserson et al. 2006). This proportional inhibition could have been due to increased drive from the reticulospinal projections, which contains both excitatory and inhibitory projections to a wide range of motoneuron pool (Riddle et al. 2009).

Another system that could provide balanced inhibition is recurrent inhibition. Recurrent inhibition is more pronounced in the proximal than distal muscles (Katz et al. 1993) and emerges more in low- than high-threshold motor units (Hultborn et al. 1988). Indeed, the duration of the recurrent inhibition in the muscles innervated by the motoneurons located in the more superior spinal cord is more prolonged than in muscles innervated by the more cephalic spinal cord regions (Bracchi et al. 1966). Therefore, increases in inhibition through either descending or recurrent pathways could result in the suppression of the activity of recruited (i.e., active) motor units while additional motor units are being recruited.

The potential role of cortico-reticulospinal pathways

The pectoralis major serves a multi-functional role, not just in assisting gross motor control of the arm (i.e. mobility in multiple directions), shoulder complex stability, and multi-joint control (i.e. glenohumeral, sternoclavicular, acromioclavicular and scapulothoracic), but also in postural maintenance, respiration, and pulmonary defensive reflexes (i.e. coughing). Due to its complex functional nature, it is likely that the brainstem pathways, such as the cortico-reticulospinal tract, play an important role in the control of this muscle alongside the corticospinal tract. The reticulospinal pathways project descending input across several spinal cord segments to the motoneurons innervating the proximal and distal muscles in both animals and humans (Colebatch et al. 1990; Davidson and Buford, 2004; 2006; Kuypers, 1981; 1982; Peterson, 1979, 1984; Shapovalov, 1972). These projections play a critical role in reaching, multi-joint postural adjustments, pulmonary defensive reflexes, and respiration (Baker, 2011; Bolser and Reier, 1998; Buford and Davidson, 2004; Lasserson et al. 2006; Mori et al. 2001; Peterson et al. 1975; Peterson, 1979; Prentice and Drew, 2001; Schepens and Drew, 2004, 2006). As such, recent findings showed that the pectoralis major may receive input from the brainstem and particularly, the reticulospinal tract (Benditt, 2006; Urfy and Suarez, 2014). Considering the key roles of the reticulospinal tract and the conceived multi-functional roles of the pectoralis major, the substantial involvement of the reticulospinal tract in the control of this muscle is plausible and should be investigated in future work.

LIMITATIONS

Some methodological limitations of the present study should be considered when interpreting the findings. In males, successful decomposition and identification of motor units depended on the participant, force level, task, and HD-sEMG array location (i.e. superior versus the inferior array). The overall sample size was low despite the relatively large number of recruited participants in experiments 1 and 2. Fewer motor units were decomposed at 25% and 50% than 15% MVF. Previously, a ~30% reduction in the number of motor units decomposed occurred for the tibialis anterior as the force level increased (Del Vecchio et al. 2020; Hassan et al. 2020). The difficulty in decomposing signals at higher force levels is primarily due to the challenges in isolating spike trains as additional motor units are recruited (Del Vecchio et al. 2020). This difficulty is amplified in the pectoralis major as motor units discharge at high and similar instantaneous rates. Second, the decomposition is highly influenced by the subcutaneous tissue thickness, composition, and muscle architecture (Del Vecchio et al. 2020; Hug et al. 2021). Considering the complex pectoralis major anatomy (Fung et al. 2009; Haladaj et al. 2019) and the variability in activation patterns (Lulic-Kuryllo et al. 2021), this may have affected the overall successful rate of the decomposition. Third, decomposition success was low for the inferior array. The exact reason is unknown but could be due to a thicker subcutaneous tissue or deeper localization of motor units. Future studies examining the lower sternocostal and abdominal regions should consider using indwelling electromyography. Lastly, challenges existed in manual editing of motor unit spike trains during the ascending part of the ramp. Attempts were made to clear the ramp-up to the best of our ability. However, the manual editing required for this part of the trapezoid was extensive, likely due to the significant variation in motor unit action potential shapes and discharge firings. Therefore, the lack of modulation observed during the ascending part of the ramp in some of the motor units shown in Figures 4A, 4B, 5A, and 6B at 15% MVF may be either the result of this limitation or the identification of motor units with relatively high force thresholds. Future studies should address these limitations and challenges in decomposition and manual editing of some pectoralis major motor units.

In females, the successful decomposition and identification of motor units were limited despite the large sample size (N = 20 in Experiment 1 and N = 9 in Experiment 2). Investigations of motor unit physiology in females using HD-sEMG is challenging, even in the muscles with simpler anatomical properties. For example, in thenar muscles, first dorsal interosseus, wrist flexors, and biceps brachii, the total number of motor units decomposed was markedly less in females than males (for examples, see Del Vecchio et al. 2020; Perreira et al. 2019). The decomposition in female pectoralis major is challenging and may be due to the breast tissue and breast composition. Future studies should consider using an HD-sEMG array with more channels to better compensate for the filtering effects of the subcutaneous and breast tissue. This may improve the results of the decomposition and enable better signal separation. Fourth, this study examined healthy young, recreationally fit individuals, and therefore, the present findings may not translate to older adults or clinical populations. Only the motor units with high accuracy (SIL > 0.9) and high cross-correlations in the tracking algorithm (> 0.8) were analyzed. These robust analyses excluded some motor units that were close to meeting the cut-off criteria but guaranteed that the motor units included in the analyses had high accuracy.

The contribution and activation of other shoulder muscles in these tasks, such as latissimus dorsi, anterior deltoid, subscapularis, teres major, coracobrachialis, and posterior deltoid, should be acknowledged, as the pectoralis major is not a sole contributor. Additionally, there exist at least two innervation zones in the pectoralis major (Barbero et al. 2012; Mancebo et al. 2019), which are challenging to isolate and would require the development of advanced signal processing techniques. The EMG amplitude quantifications, therefore, involved averaging across the innervation zones. The involvement of additional shoulder muscles and averaging across innervation zones may explain the low increase in EMG amplitudes documented at 15% and

25% MVF. Lastly, we did not acquire task-specific MVF at the end of the Experiment 1 as we did in Experiment 2. Therefore, the influence of fatigue cannot be discounted. However, considering the participants did not experience fatigue following Experiment 2, both experiments were of similar length and had a fairly similar experimental protocol, we do not believe fatigue influenced our EMG amplitude or motor unit discharge rate findings.

CONCLUSIONS

The neural control of the pectoralis major muscle was explored in several tasks across varying force levels. Using motor unit tracking, we showed for the first-time clear saturation of motor units in the pectoralis major, suggesting that the main control strategy of this muscle relies on motor unit recruitment to modulate increases in force. Moreover, we showed that the motor units in this muscle have a high discharge rate in relatively low contractions, which compare to those previously reported at maximal voluntary contractions (Bracchi et al. 1966). Collectively, these findings suggest the pectoralis major relies on motor unit recruitment as the predominant motor control strategy to increase force. The absence of rate coding in the sustained hold may be because the motoneurons innervating the pectoralis major are influenced by strong persistent inward currents, balanced inhibition, or recurrent inhibition. These findings have implications in understanding the neural control of more proximal muscles of the upper limb and lay the groundwork for a more deliberate investigation into the neural control of these muscles.

ACKNOWLEDGMENTS

This research was partially funded through an NSERC Discovery Grant held by Dr. Clark R. Dickerson (311895-2016). The equipment used was funded through combined support from the

Canada Foundation for Innovation and the Ontario Research Fund. Dr. Dickerson is also funded as an NSERC-sponsored Canada Research Chair in Shoulder Mechanics. Tea Lulic-Kuryllo was supported by the Ontario Graduate Scholarship.

CONTRIBUTIONS

T.L.-K, J.N, F.N. and C.R.D. conceived and designed research; T.L.-K performed experiments; T.L.-K., C.K.T., J.N., F.N., and C.R.D. interpreted results of experiments; T.L.-K prepared figures; T.L.-K., C.K.T., F.N., and C.R.D. drafted manuscript; T.L.-K., C.K.T., J.N., F.N., and C.R.D. edited and revised manuscript; T.L.-K., C.K.T., J.N., F.N., and C.R.D. approved final version of manuscript; T.L.-K and F.N. analyzed data.

References

1. **Ackland CD, Pak P, Richardson M, Pandy MG**. Moment arms of the muscles crossing the anatomical shoulder. *Journal of Anatomy*, 213: 383-390, 2008.

2. **Ackland CD, Pandy MG.** Moment Arms of the Shoulder Muscles during Axial Rotation. *Journal of Orthopaedic Research*, 29(5): 658-667, 2011.

3. **Afsharipour B, Manzur N, Duchcherer J, Fenrish KF, Thompson CK, Negro F, Quinlan KA, Bennett DJ, Gorassini MA.** Estimation of self-sustained activity produced by persistent inward currents using firing rate profiles of multiple motor units in humans. *J Neurophysiol*, 124(1): 63-85, 2020.

4. **de Almeida ATR, Kirkwood PA.** Multiple phases of excitation and inhibition in central respiratory drive potentials of thoracic motoneurones in the rat. *J Physiol*, 588(Pt 15): 2731-44, 2010.

5. **Baker SN.** The primate reticulospinal tract, hand function and functional recovery. *Journal of Physiology*, 589 (23): 5603-5612, 2011.

6. **Banditt JO.** The neuromuscular respiratory system: physiology, pathophysiology, and a respiratory care approach to patients. *Respir Care*, 51(8): 829-37, 2006.

7. **Barbero M, Merletti R, Rainoldi A.** Upper Limb. Atlas of Muscle Innervation Zones. Understanding Surface Electromyography and Its Applications. Springer-Verlag Mailand; 2012: 103-120.

8. **Berg RW, Alaburda A, Hounsgaard J.** Balanced inhibition and excitation drive spike activity in spinal half-centers. *Science*, 315(5810): 390-3, 2007.

9. **Binder MD, Powers RK, Heckman CJ.** Nonlinear Input-Output Functions of Motoneurons. *Journal of Physiology*, 35(1): 31-39, 2020.

10. **Boccia G, Martinez-Valdes E, Negro F, Rainoldi A.** Motor unit discharge rate and the estimated synaptic input to the vasti muscles is higher in open compared with closed kinetic chain exercise. *J Appl Physiol* 127(4): 950-958, 2019.

11. **Bolser DC, Reier PJ.** Inspiratory and expiratory patterns of the pectoralis major muscle during pulmonary defensive reflexes. *Journal of Applied Physiology*, 85(5): 1786-1792, 1998.

12. **Bracchi F, Decandia M, Gualtierotti T.** Frequency stabilization in the motor centers of spinal cord and caudal brain stem. *Am J Physiol* 210: 1170–1177, 1966.

13. **Brown JMM, Wickham JB, McAndrew DJ, Huang X-F.** Muscles within muscles: Coordination of 19 muscle segments within three shoulder muscles during isometric tasks. *Journal of Electromyography and Kinesiology*, 17(1): 57-73, 2007.

14. **Brownstone RM.** Beginning at the end: repetitive firing properties in the final common pathway. *Prog Neurobiol*, 78: 156-172, 2006.

15. **Buford JA, Davidson AG.** Movement-related and preparatory activity in the reticulospinal system of the monkey. *Exp Brain Res,* 159: 284–300, 2004.

16. **Caroll TJ, Selvanayagam VS, Riek S, Semmler JG.** Neural adaptations to strength training: Moving beyond transcranial magnetic stimulation and reflex studies. *Acta Physiol (Oxf)*, 202(2): 119-40, 2011.

17. **Cogliati M, Cudicio A, Martinez-Valdes E, Tarperi C, Schena F, Orizio C, Negro F.** Half marathon induces changes in central control and peripheral properties of individual motor units in master athletes. *J Electromyogr Kinesiol* 55: 102472, 2020.

18. **Colebatch JG, Rothwell JC, Day BL, Thompson PD, Marsden CD.** Cortical outflow to proximal arm muscles in man. *Brain*, 113: 1843-1856, 1990.

19. **Davidson AG, Buford JA.** Motor outputs from the primate reticular formation to shoulder muscles as revealed by stimulus triggered averaging. *J Neurophysiol*, 92:83–95, 2004.

20. **Davidson AG, Buford JA**. Bilateral actions of the reticulospinal tract on arm and shoulder muscles in the monkey: stimulus triggered averaging. *Exp Brain Res*,173:25–39, 2006.

21. **De Luca CJ, LeFever RS, McCue MP, Xenakis AP.** Behaviour of human motor units in different muscles during linearly varying contractions. J Physiol 329: 113–128, 1982.

22. **De Luca CJ.** Control Properties of Motor Units. *Journal of Experimental Biology*, 115: 125-136, 1985.

23. **Del Vecchio A, Holobar A, Falla D, Felici F, Enoka RM, Farina D.** Tutorial: Analysis of motor unit discharge characteristics from high-density surface EMG signals. Journal of Electromyography and Kinesiology, 53: 102426, 2020.

24. **Elliott HC.** Studies on the motor cells of the spinal cord. I. Distribution in the normal human cord. *Am J Anat*, 70: 95-117, 1942.

25. **Farina D, Merletti R, Enoka RM.** The extraction of neural strategies from the surface EMG. *Journal of Applied Physiology*, 96(4): 1486-1495, 2004.

26. **Fuglevand AJ, Lester RA, Johns RK.** Distinguishing intrinsic from extrinsic factors underlying firing rate saturation in human motor units. *Journal of Neurophysiology*, 113(5): 1310-22, 2015.

27. **Fung L, Wong B, Ravichandiran K, Agur A, Rindlisbacher T, Elmaraghy A.** Three-Dimensional Study of Pectoralis Major Muscle and Tendon Architecture. *Clinical Anatomy*, 22: 500-508, 2009.

28. **Haladaj R, Wysiadecki G, Clarke E, Polguj M, Topol M.** Anatomical Variations of the Pectoralis Major Muscle: Notes on Their Impact on Pectoral Nerve Innervation Patterns and Discussion on Their Clinical Relevance. *Biomed Research International*, 2019, doi: 10.1155/2019/6212039.

29. **Hassan A, Thompson CK, Negro F, Cummings M, Powers RK, Heckman CJ, Dewald JPA, McPherson LM.** Impact of parameter selection on estimates of motoneuron excitability using paired motor unit analysis. *Journal of Neural Engineering*, 2020.

30. **Heckman CJ, Mottram C, Quinlan K, Theiss R, Schuster J.** Motoneuron excitability: the importance of neuromodulatory inputs. *Clinical Neurophysiology*, 120: 2040-2054, 2009.

31. **Hug F, Avrillon S, Del Vecchio A, Casolo A, Ibanez J, Nuccio S, Rossato J, Holobar A, Farina D.** Analysis of motor unit spike trains estimated from high-density surface electromyography is highly reliable across operators. *J Electromyogr Kinesiol*, 58: 102548, 2021.

32. **Hultborn H, Katz R, Mackel R.** Distribution of recurrent inhibition within a motor nucleus. II. Amount of recurrent inhibition in motoneurones to fast and slow units. *Acta Physiol Scand*, 134: 363-374, 1988.

33. **Johnson MD, Heckman CJ.** Gain control mechanisms in spinal motoneurons. *Front. Neural Circuits*, 8: 81, 2014.

34. **Johnson MD, Heckman CJ.** Interactions between focused synaptic inputs and diffuse neuromodulation in the spinal cord. *Ann N Y Acad Sci*, 1198: 35-41, 2010.

35. **Kanosue K., Yoshida M, Akazawa K, Fujii K.** The Number of Active Motor Units and Their Firing Rates in Voluntary Contraction of Human Brachialis Muscle. *Japanese Journal of Physiology,* 29: 427-443, 1979.

36. **Katz R, Mazzocchio R, Penicaud A, Rossi A.** Distribution of recurrent inhibition in the human upper limb. *Acta Physiol Scand*, 149: 183-189, 1993.

37. **Kukulka CG, Clamann HP.** Comparison of the recruitment and discharge properties of motor units in human brachial biceps and adductor pollicis during isometric contractions. *Brain Research*, 219: 45-55, 1981.

38. **Kuypers HG** (1981) Anatomy of the descending pathways. In: Handbook of physiology—the nervous system II (Brookhart JM, Mountcastle VB, eds), pp 597–666. Bethesda, MD: American Physiological Society.

39. **Kuypers HG.** A new look at the organization of the motor system. *Progress in Brain Research*, 57: 381-403, 1982.

40. **Lasserson D, Mills K, Arunachalam R, Polkey M, Moxham J, Kalra L.** Differences in motor activation of voluntary and reflex cough in humans. *Thorax*, 61(8): 699-705, 2006.

41. **Lee RH, Heckman CJ.** Bistability in spinal motoneurons in vivo: systematic variations in persistent inward currents. *Journal of Neurophysiology*, 80(2): 583-593, 1998.

42. **Leonardis JM, Desmet DM, Lipps DB.** Quantifying differences in the material properties of the fiber regions of the pectoralis major using ultrasound shear wave elastography. *Journal of Biomechanics*, 63: 41-46, 2017.

43. **Lulic-Kuryllo T, Negro F, Jiang N, Dickerson CR.** Standard bipolar surface EMG estimations mischaracterize pectoralis major activity in commonly performed tasks. *Journal of Electromyography and Kinesiology*, 56: 102509, 2021.

44. **Maganaris CN, Baltzopoulos V, Sargeant AJ.** Repeated contractions alter the geometry of human skeletal muscle. Journal of Applied Physiology 93(6): 2089-2094, 2002.

45. **Mancebo F, Cabral HV, de Souza LML, de Oliveira LF, Vieira TM**. Innervation zone locations distribute medially within the pectoralis major muscle during bench press exercise. *Journal of Electromyography and Kinesiology*, 46: 8-13, 2019.

46. **Marata R, Fenrich KK, Zhao E, Neuber**-Hess MS, Rose KP. Distribution and Density of Contacts From Noradrenergic and Sertonergic Boutons on the Dendrites of Neck Flexor Motoneurons in the Adult Cat. *J Comp Neurol,* 523(11): 1701-16, 2015.

47. **Martinez-Valdes E, Negro F, Laine CM, Falla D, Mayer F, Farina D.** Tracking motor units longitudinally across experimental sessions with high-density electromyography. *The Journal of Physiology*, 595(5): 1479-1496, 2017.

48. **Martinez-Valdes E, Falla D, Negro F, Mayer F, Farina D.** Differential Motor Unit Changes after Endurance or High-Intensity Interval Training. *Med Sci Sports Exerc*, 49(6): 1126-1136, 2017.

49. **Martinez-Valdes E, Negro F, Falla D, De Nunzio AM, Farina D.** Surface electromyographic amplitude does not identify differences in neural drive to synergistic muscles. *Journal of Applied Physiology*, 124(4): 1071-1079, 2018.

50. **Milner-Brown HS, Stein RB, Yemm R.** Changes in firing rate of human motor units during linearly changing voluntary contractions. *Journal of Physiology*, 230: 371-390, 1973.

51. **Monster AW, Chan H.** Isometric force production by motor units of extensor digitorum communis muscle in man. *Journal of Neurophysiology,* 40: 1432-1443, 1977.

52. **Montague SJ, Fenrich KK, Mayer-Macaulay C, Maratta R, Heuber-Hess MS, Rose KP.** Nonuniform Distribution of Contacts From Noradrenergic and Serotonergic Boutons on the Dendrites of Cat Splenius Motoneurons. *J Comp Neurol,* 521(3): 638-56, 2013.

53. **Mori S, Matsuyama K, Mori F, Nakajima K**. Supraspinal sites that induce locomotion in the vertebrate central nervous system. *Adv Neurol*, 87:25– 40, 2001.

54. **Negro F, Muceli S, Castronovo AM, Holobar A, Farina D.** Multi-channel intramuscular and surface EMG decomposition by convolutive blind source separation. Journal of Neural Engineering, 13 (2): 026027, 2016.

55. **Paton ME, Brown JMM.** An Electromyographic Analysis of Functional Differentiation in Human Pectoralis Major Muscle. *Journal of Electromyography and Kinesiology*, 4(3): 161-169, 1994.

56. **Pereira HM, Schlinder-DeLap B, Keenan KG, Negro F, Farina D, Hyngstrom AS, Nielson KA, Hunter SK.** Oscillations in neural drive and age-related reductions in force steadiness with a cognitive challenge. *Journal of Applied Physiology*, 126(4): 1056-1065, 2019.

57. **Peterson BW, Maunz RA, Pitts NG, Mackel RG.** Patterns of projection and branching of reticulospinal neurons. *Experimental Brain Research*, 23: 333-351, 1975.

58. **Peterson BW.** Reticulospinal projections to spinal motor nuclei. *Annual Review of Physiology*, 41: 127-40, 1979.

59. **Peterson BW, Pitts NG, Fukushima K.** Reticulospinal Connections with Limb and Axial Motoneurons. *Experimental Brain Research*, 36: 1-20, 1979.

60. **Peterson B. W.** (1984). “The reticulospinal system and its role in the control of movement,” in Brainstem Control of Spinal Cord Function, ed. Barnes C. D. (New York, NY: Academic Press), 27–86.

61. **Piervirgili G., Petracca F, Merletti R.** A new method to assess skin treatments for lowering the impedance and noise of individual gelled Ag-AgCl electrodes. *Physiol Meas*, 35(10): 2101-18, 2014.

62. **Powers RK, Heckman CJ.** Synaptic control of the shape of the motoneuron pool input-output function. *J Neurophysiol*, 117(3): 2017.

63. **Prentice SD, Drew T.** Contributions of the reticulospinal system to the postural adjustments occurring during voluntary gait modifications. *J Neurophysiol*, 85:679–698, 2001.

64. **Riddle CN, Edgley S, Baker SN.** Direct and indirect connections with upper limb motoneurons from the primate reticulospinal tract. *J Neurosci*, 29: 4993-4999, 2009.

65. **Schepens B, Drew T**. Independent and convergent signals from the pontomedullary reticular formation contribute to the control of posture and movement during reaching in the cat. *J Neurophysiol*, 92:2217–2238, 2004.

66. **Schepens B, Drew T.** Descending signals from the pontomedullary reticular formation are bilateral, asymmetric, and gated during reaching movements in the cat. *J Neurophysiol*, 96:2229 –2252, 2006.

67. **Seki K, Narusawa M.** Firing rate modulation of human motor units in different muscles during isometric contraction with various forces. *Brain Research*, 719(1-2): 1-7: 1996.

68. **Shapovalov AI.** Extrapyramidal monosynaptic and disynaptic control of mammalian alpha-motoneurons. *Brain Res*, 40:105–115, 1972.

69. **Thompson CK, Negro F, Johnson MD, Holmes MR, McPherson LM, Powers RK, Farina D, Heckman CJ.** Robust and accurate decoding of motoneuron behavior and prediction of the resulting force output. *Journal of Physiology*, 596(14): 2643-2659, 2018.

70. **Urfy MZ, Suarez JI.** Chapter 17 – Breathing and the nervous system. *Handbook of Clinical Neurology*, 119: 241-250, 2014.

71. **Vanderhorst VGJM, Holstege G.** Organization of Lumbosacral Motoneuronal Cell Groups Innervating Hindlimb, Pelvic Floor, and Axial Muscles in the Cat. *J Comp Neurol*, 382(1): 46-76, 1997.

72. **Walton C, Kalmar JM, Cafarelli E.** Effect of caffeine on self-sustained firing in human motor units. *J Physiol*, 545(2): 671-679, 2002.

73. **Westgaard RH, De Luca CJ.** Motor control of low-threshold motor units in the human trapezius muscle. *Journal of Neurophysiology*, 85(4): 1777-1781, 2001.

74. **Wickham JB, Brown JMM, McAndrew DJ.** Muscles within muscles: Anatomical and functional segmentation of selected shoulder joint musculature. *Journal of Musculoskeletal Research*, 8(1): 57-73, 2004.

75. **Wickham JB, Brown JM.** The function of neuromuscular compartments in human shoulder muscles. *Journal of Neurophysiology*, 107(1): 336-45, 2012.

76. **Wilson JM, Thompson CK, Miller LC, Heckman CJ.** Intrinsic excitability of human motoneurons in biceps brachii versus triceps brachii. *Journal of Neuroscience*, 113(10): 3692-3699, 2015.

77. **Wolfe SW, Wickiewicz TL, Cavanaugh JT.** Ruptures of the pectoralis major muscle. *The American Journal of Sports Medicine*, 20(5): 309-312, 1992.

Figure Captions

Figure 1: HD-sEMG array positioning and experimental data analyses. **A:** Two HD-sEMG arrays were positioned on the pectoralis major in males and females. Top array (i.e. superior array) was located ~ 2 cm inferior to the clavicle. Bottom array (i.e. inferior array) was located directly below the superior array. **B:** Example of raw force traces in 15%, 25%, and 50% MVF (left) and raw HD-sEMG signals in a single trial (right). **C:** Example of motor unit matching based on motor unit action potential shape (left) and instantaneous discharge rate of a single motor unit matched at 15% and 25% MVF. Figure on the left also shows the corresponding force trace at 15% and 25% MVF.

Figure 2: Experiment 1 consisted of four tasks: adduction 60°, which required isometric ramp and hold towards the sternum at 60° of abduction (A); adduction 90°, which required isometric ramp and hold towards the sternum at 90° of abduction (B); adduction external 90°, which required isometric ramp and hold towards the sternum at 90° of abduction and 90° of external rotation (C); and internal rotation 60°, which required isometric ramp and hold by medially rotating the arm towards the sternum at 60° of abduction (D). Experiment 2 consisted of two tasks: flexion, which required isometric ramp and hold pushing forward at ~20° of abduction (E), and horizontal adduction, which required isometric ramp and hold pushing across the body at 90° of elevation and ~ 50° of plane of elevation (F).

Figure 3: Examples of two motor units with instantaneous discharge rates at 15% and 25% MVF in adduction 60° (**A**) and internal rotation 60° (**B**) in males with corresponding cross-correlations and motor unit action potential signatures. Each colour represents the discharge rate of the same motor unit in 15% (blue) and 25% MVF (red).

Figure 4: Examples of two motor units with instantaneous discharge rates at 15% and 25% MVF in adduction 90° (**A**) and flexion (**B**) in males with corresponding cross-correlations and motor unit action potential signatures. Each colour represents the discharge rate of the same motor unit in 15% (blue) and 25% MVF (red).

Figure 5: Examples of two motor units in horizontal adduction with instantaneous discharge rates at 15% and 25% MVF (**A**) or 25% and 50% MVF (**B**) in males with corresponding cross-correlations and motor unit action potential signatures. Each colour represents the discharge rate of the same motor unit in 15% (blue) and 25% MVF (red).

Figure 6: Examples of two motor units and their instantaneous discharge rates in adduction 90° and adduction external 90 at 15% and 25% MVF in females with motor unit action potential signatures and cross-correlations. **A:** Representative example of one motor unit in adduction 90°, showing instantaneous discharge rate across time at 15% and 25% MVF. **B:** Same motor unit displayed in A with force overlayed for 15% and 25% MVF. **C:** Motor unit action potentials obtained from high-density sEMG signals corresponding to the same motor unit displayed (A). **D:** Representative example of one motor unit in adduction external 90 (ADER90), showing

instantaneous discharge rate across time at 15% and 25% MVF. **E:** Same motor unit displayed in D with force overlayed for 15% and 25% MVF. **F:** Motor unit action potentials obtained from high-density sEMG signals corresponding to the same motor unit displayed in top panel (D).

Competing interests

All authors declare no conflict of interest.

Data Availability Statement

The data that support the findings of this study are available from the corresponding author upon reasonable request.

Tables with table captions

Table 1: Summary of mean force (± standard deviation) represented in Newtons and as a percentage of MVF exerted by the *male* participants across tasks and force levels, including the maximal voluntary force. Observed Force: mean force in Newtons achieved during the sustained hold. Observed %MVF: mean force achieved during sustained hold depicted as a percentage.

Task	Required Force Level	Observed Force (N)	Observed %MVF
Adduction 60	15%	45.7 ± 6.1	15.7 ± 0.75
	25%	75.6 ± 10.3	26.1 ± 1.7
	100%	290.1 ± 38.9	-
Adduction 90	15%	48.4 ± 20.1	15.2 ± 2.2
	25%	79.5 ± 29.9	25 ± 1.6
	100%	314.7 ± 112.5	-
Internal Rotation	15%	44.7 ± 11.7	15.2 ± 1.7
	25%	74.3 ± 17.3	25.5 ± 1.9
	100%	290.7 ± 64.4	-
Flexion	15%	25.4 ± 7.4	13.6 ± 1.1
	25%	45.1 ± 12.4	24.2 ± 1.2
	100%	185.4 ± 45.9	-
Horizontal Adduction	15%	39.1 ± 13.1	16.8 ± 1
	25%	63.4 ± 21.8	27.3 ± 1.6
	50%	110.4 ± 38.7	53.5 ± 1.9
	100%	233.7 ± 86	-

Table 2: Summary of motor unit physiology in male participants in adduction 60, internal rotation, adduction 90, flexion, and horizontal adduction at 15% and 25% MVF. 50% MVF is also reported for horizontal adduction. The number of motor units, including the number of participants, successfully decomposed, is included in column 3. Mean discharge rate and CoV inter-spike interval with standard deviation for each task and force level is also reported. Statistical analyses between 15% and 25% MVF within a task for EMG amplitude, discharge rate, and coefficient of variation are reported in columns 7 through 9. Bolded numbers denote significant differences between force levels within a task. DR: discharge rate; CoV: coefficient of variation.

Task	Force level (%MVF)	Number of motor units (Number of participants)	Mean EMG amplitude (%MVF)	Statistical comparisons (EMG amplitude)	Mean DR across sustained hold (pps)	Statistical comparisons (DR)	Coefficient of Variation	Statistical comparisons (CoV)	Mean DR in the first 5 seconds of the sustained hold (pps)
Adduction 60	15	13 (N = 8)	8.5 ± 3.3	**t_7 = -4.07, p = 0.004, *d* = 1.42**	13.8 ± 2.4	t_7 = -0.65, p = 0.53	15.9 ± 2.7	t_7 = -2.16, p = 0.06	14.2 ± 2.6
	25	13 (N = 8)	13.3 ± 5		14.4 ± 1.4		19.1 ± 4		15.2 ± 2.2
Internal rotation 60	15	16 (N = 6)	9.1 ± 6.4	**t_5 = -4.38, p = 0.007**	13.9 ± 1.1	t_5 = -0.83, p = 0.44	18.2 ± 3.4	t_5 = -1.23, p = 0.27	14.6 ± 0.4
	25	16 (N = 6)	13 ± 4.9		14.5 ± 1		19.1 ± 2.4		15 ± 1.7
Adduction 90	15	16 (N = 7)	6.5 ± 3.9	**t_6 = -4.24, p = 0.005, *d* = 1.58**	12 ± 3.6	t_6 = -0.38, p = 0.71	21.1 ± 5.7	t_6 = 0.50, p = 0.63	12.7 ± 4
	25	16 (N = 7)	10.8 ± 3.8		12.3 ± 3.4		19.7 ± 5.7		12.9 ± 3.2
Flexion	15	13 (N = 5)	11.7 ± 6.5	**t_4 = -7.66, p = 0.001, *d* = 3.14**	13.2 ± 1.6	t_4 = -0.92, p = 0.41	18.5 ± 4	t_4 = -0.41, p = 0.69	14.6 ± 2.1
	25	13 (N = 5)	16.1 ± 5.5		13.9 ± 1.6		19.4 ± 4.2		16.4 ± 1.7
Horizontal adduction	15	19 (N = 6)	9.2 ± 3.3	**t_4 = -5.42, p = 0.005**	14.6 ± 2.5	t_5 = 2.44; p = 0.058	15.9 ± 3.1	t_5 = -2.58, p = 0.049	17.5 ± 3.2
	25	19 (N = 6)	14.3 ± 4.5		12.9 ± 2.4		21.8 ± 5.7		16.1 ± 3.1
Horizontal adduction	25	23 (N = 4)	12.3 ± 4.9		13.7 ± 2.7	t_3 = -2.20, p = 0.11	16.7 ± 4.4	t_3 = -2.02, p = 0.13	16.1 ± 1.6
	50	23 (N = 4)	27.7 ± 10.8		15.9 ± 2.8		19.7 ± 2.2		18.7 ± 3.6

Table 3: Summary of motor unit physiology in *female* participants in adduction 90, internal rotation, and adduction external 90 tasks at 15% and 25% MVF. The number of motor units, including the number of participants, successfully decomposed is included in column 3. Mean discharge rate, Coefficient of Variation (with standard deviation) for each task, and force level is also reported.

Task	Force Level (%MVF)	Number of Motor Units (Number of Participants)	Discharge Rate (pps)	Coefficient of Variation
Adduction 90	15	18 (N = 5)	9.4 ± 1.3	17.3 ± 2.1
	25	4 (N = 3)	9 ± 2.1	19.7 ± 4.1
Internal Rotation 60	15	5 (N = 2)	14.8 ± 1.2	14.1 ± 0.8
	25	1 (N = 1)	12.1	15.9
Adduction External 90	15	10 (N = 2)	8.8 ± 0.6	17.9 ± 0.5
	25	9 (N = 3)	9.9 ± 0.6	17 ± 1.5

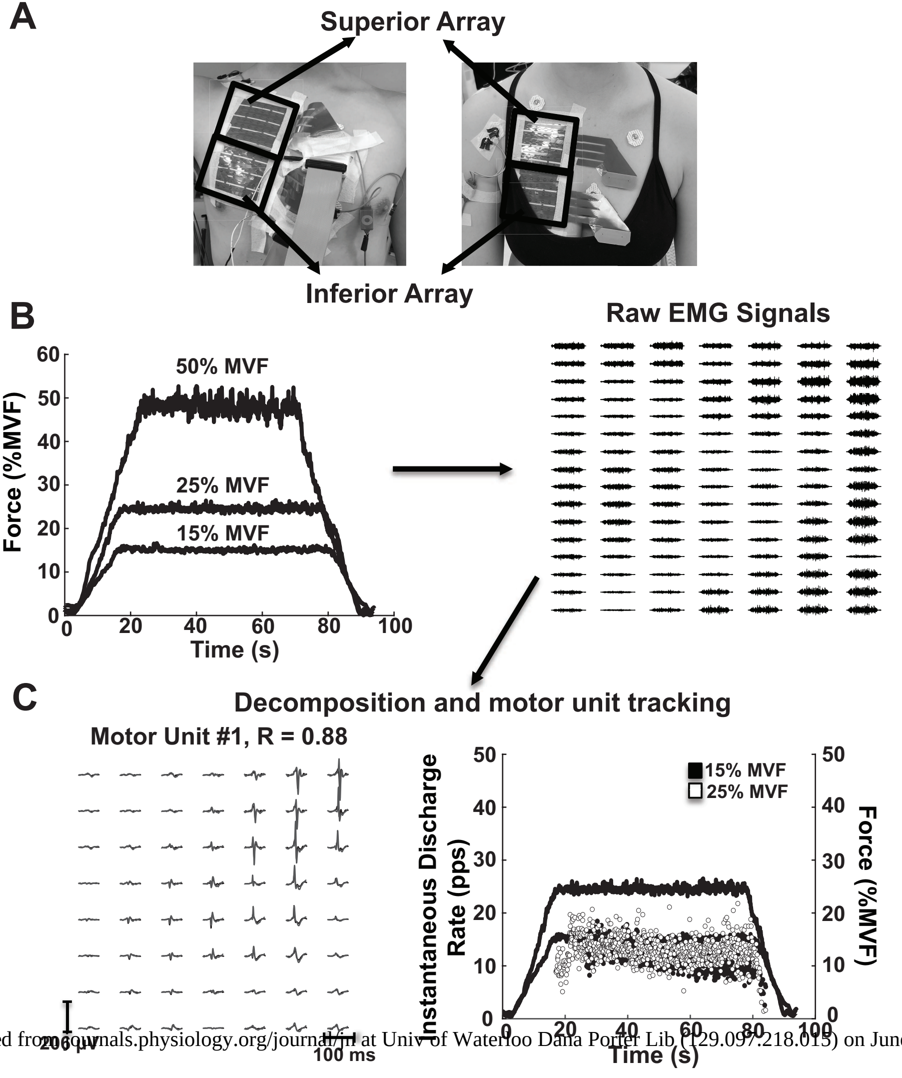
A
Superior Array
Inferior Array
B
Raw EMG Signals
50% MVF
25% MVF
15% MVF
Force (%MVF)
Time (s)
C
Decomposition and motor unit tracking
Motor Unit #1, R = 0.88
15% MVF
25% MVF
Instantaneous Discharge Rate (pps)
Force (%MVF)
Time (s)
200 µV
100 ms

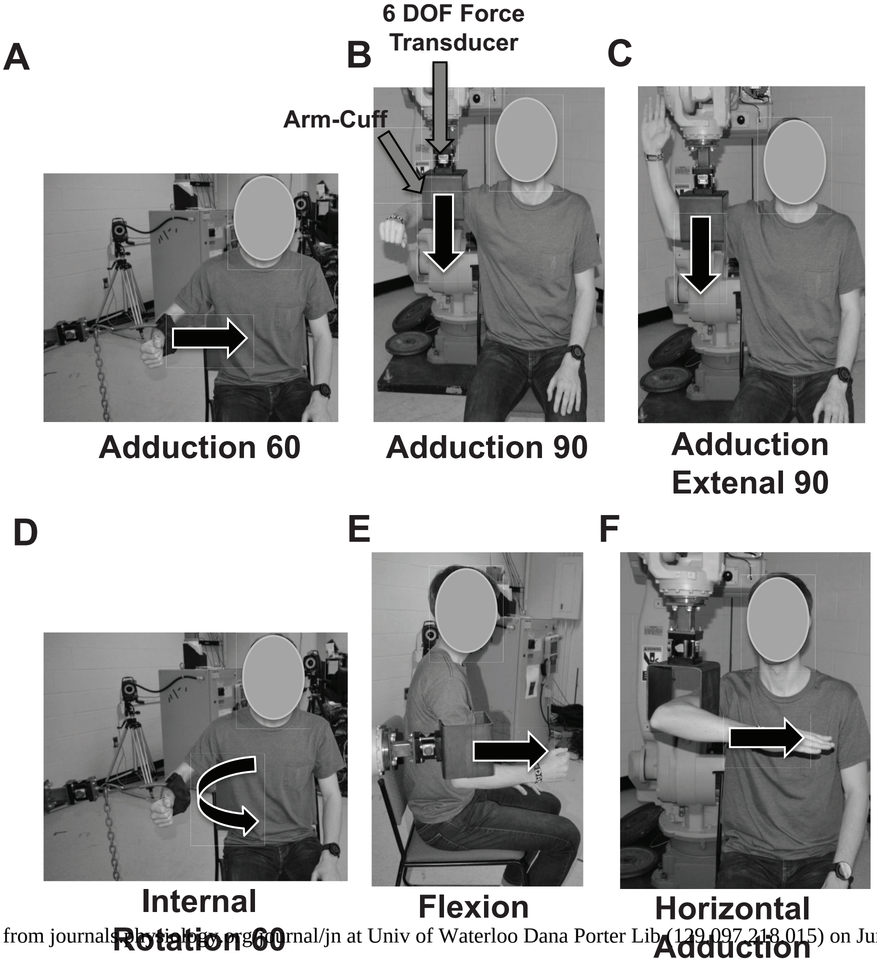
A
B
C
6 DOF Force Transducer
Arm-Cuff
Adduction 60
Adduction 90
Adduction Extenal 90
D
E
F
Internal Rotation 60
Flexion
Horizontal Adduction

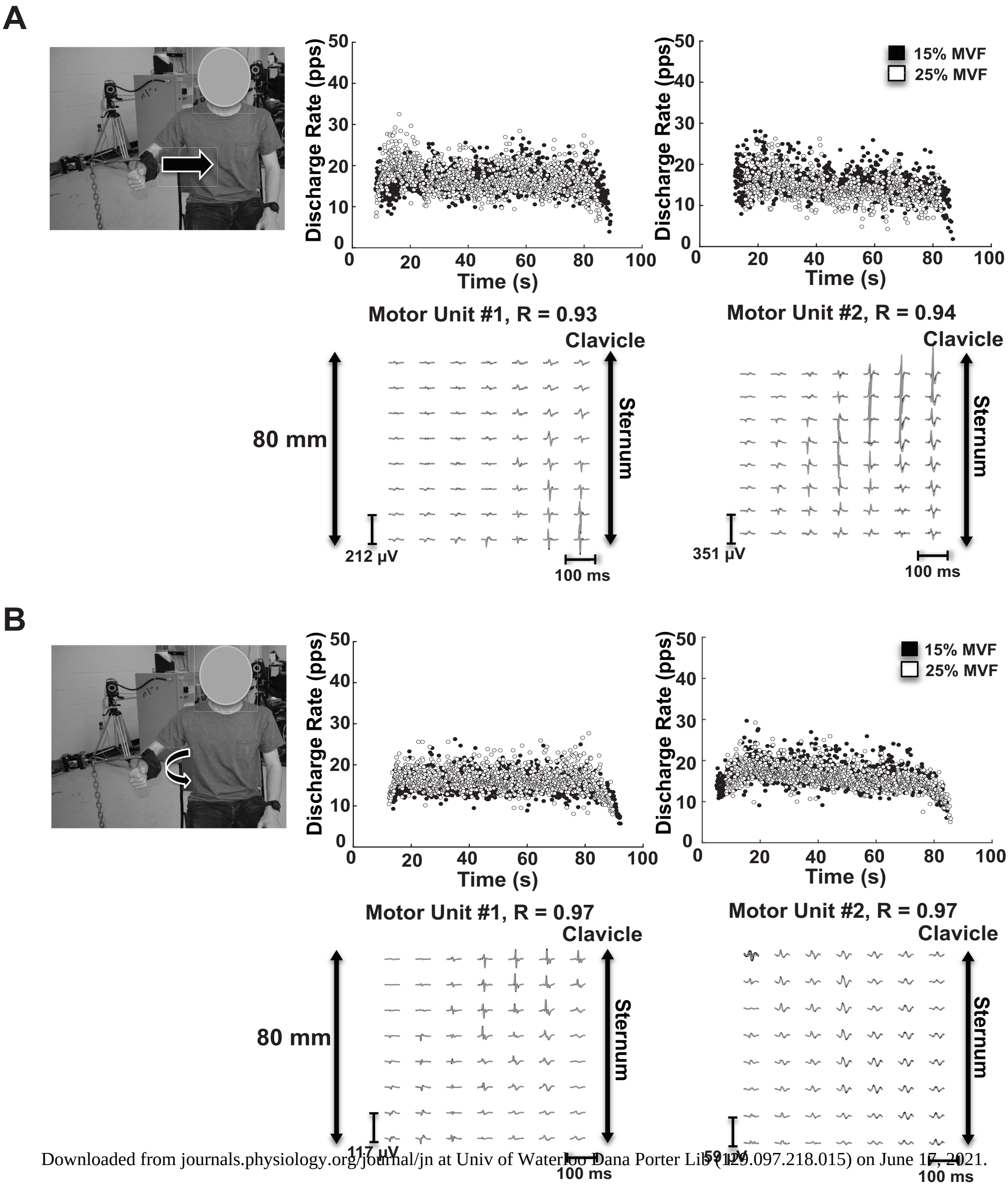

A
Discharge Rate (pps)
Time (s)
15% MVF
25% MVF
Motor Unit #1, R = 0.93
Motor Unit #2, R = 0.94
Clavicle
Sternum
80 mm
212 µV
351 µV
100 ms
B
Motor Unit #1, R = 0.97
Motor Unit #2, R = 0.97
117 µV
100 ms

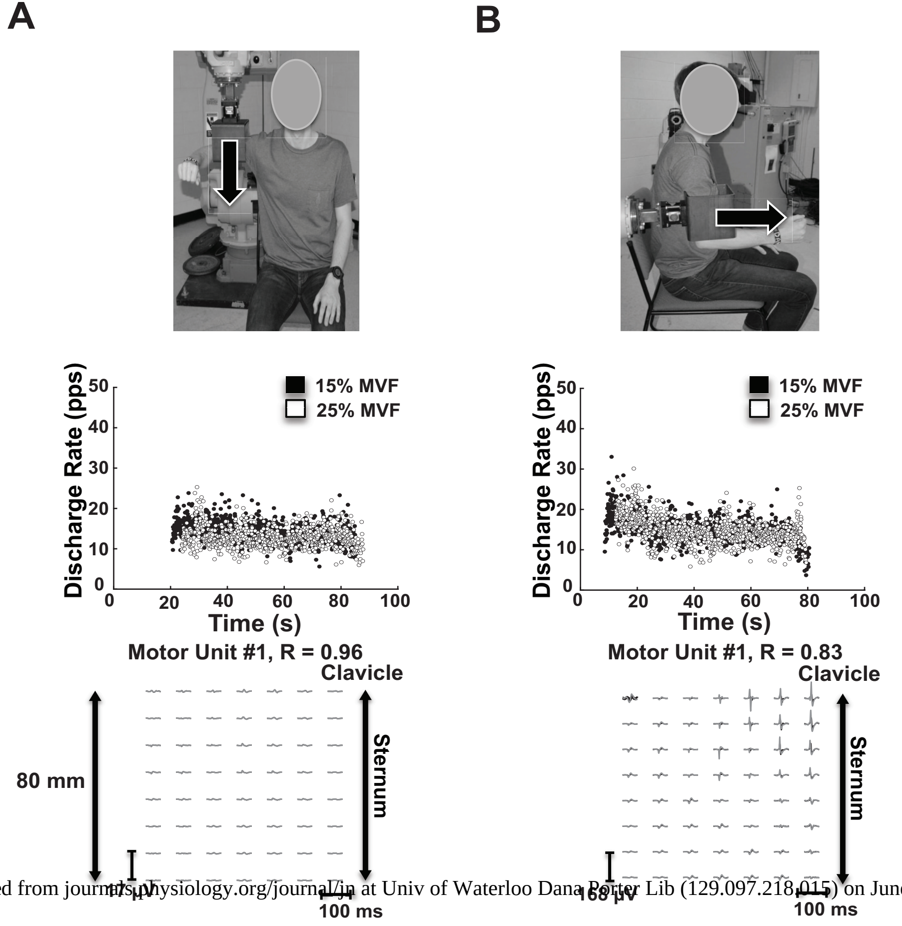
A
15% MVF
25% MVF
Discharge Rate (pps)
Time (s)
Motor Unit #1, R = 0.96
Clavicle
Sternum
80 mm
100 ms
B
15% MVF
25% MVF
Discharge Rate (pps)
Time (s)
Motor Unit #1, R = 0.83
Clavicle
Sternum
168 µV
100 ms

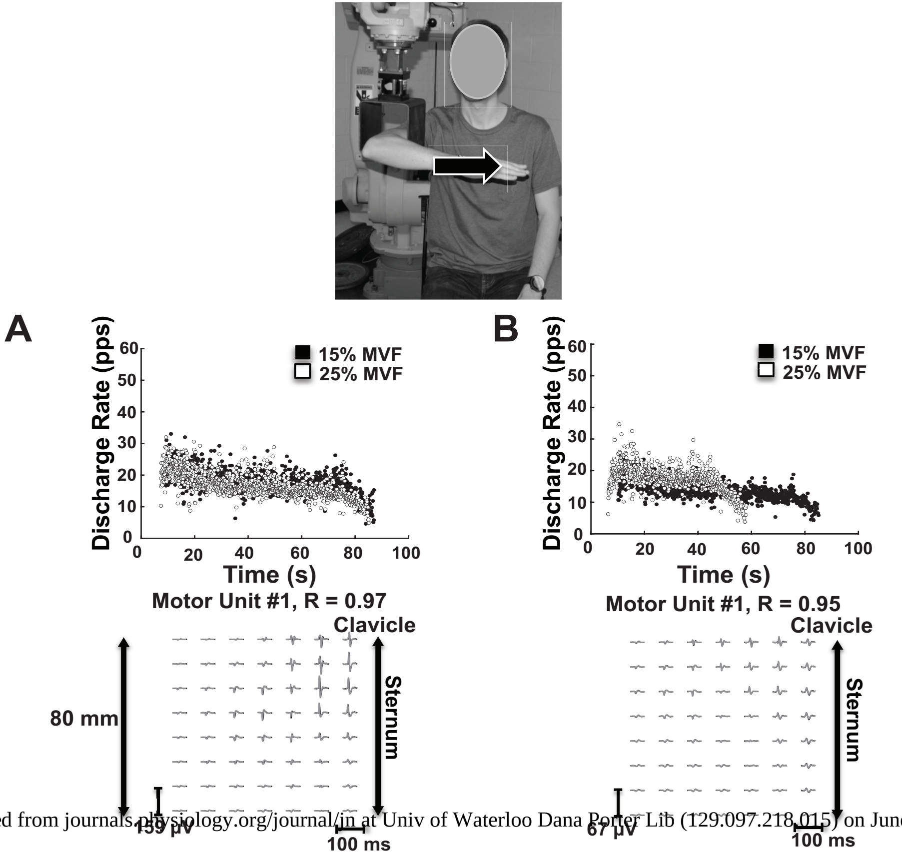
A
Discharge Rate (pps)
60
50
40
30
20
10
0
15% MVF
25% MVF
0
20
40
60
80
100
Time (s)
Motor Unit #1, R = 0.97
Clavicle
Sternum
80 mm
100 ms
B
Discharge Rate (pps)
60
50
40
30
20
10
0
15% MVF
25% MVF
0
20
40
60
80
100
Time (s)
Motor Unit #1, R = 0.95
Clavicle
Sternum
67 µV
100 ms

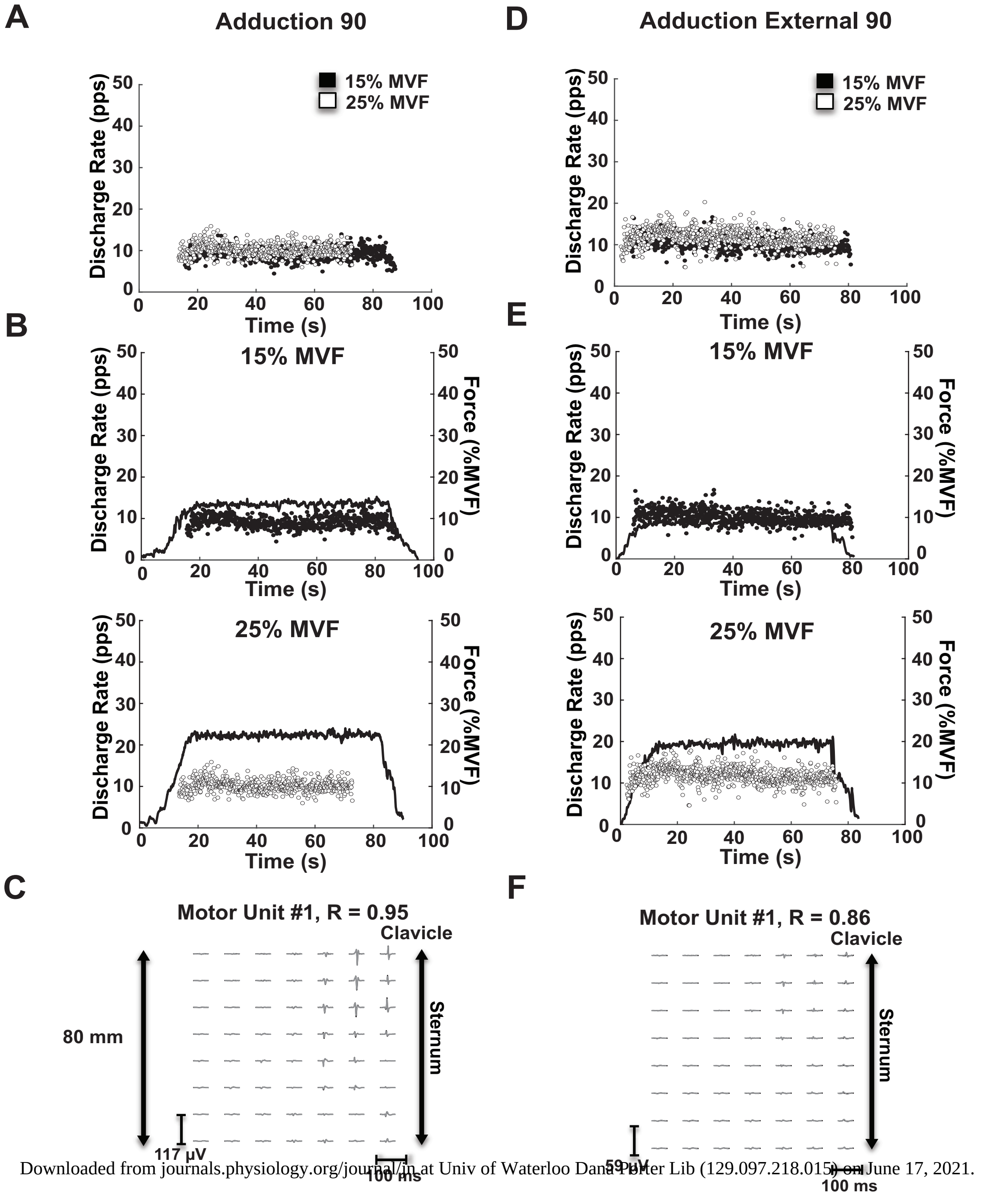

A
Adduction 90
15% MVF
25% MVF
Discharge Rate (pps)
Time (s)
B
15% MVF
25% MVF
Force (%MVF)
C
Motor Unit #1, R = 0.95
Clavicle
Sternum
80 mm
117 µV
100 ms
D
Adduction External 90
E
F
Motor Unit #1, R = 0.86
59 µV

Table 1: Summary of mean force (± standard deviation) represented in Newtons and as a percentage of MVF exerted by the *male* participants across tasks and force levels, including the maximal voluntary force. Observed Force: mean force in Newtons achieved during the sustained hold. Observed %MVF: mean force achieved during sustained hold depicted as a percentage.

Task	Required Force Level	Observed Force (N)	Observed %MVF
Adduction 60	15%	45.7 ± 6.1	15.7 ± 0.75
	25%	75.6 ± 10.3	26.1 ± 1.7
	100%	290.1 ± 38.9	-
Adduction 90	15%	48.4 ± 20.1	15.2 ± 2.2
	25%	79.5 ± 29.9	25 ± 1.6
	100%	314.7 ± 112.5	-
Internal Rotation	15%	44.7 ± 11.7	15.2 ± 1.7
	25%	74.3 ± 17.3	25.5 ± 1.9
	100%	290.7 ± 64.4	-
Flexion	15%	25.4 ± 7.4	13.6 ± 1.1
	25%	45.1 ± 12.4	24.2 ± 1.2
	100%	185.4 ± 45.9	-
Horizontal Adduction	15%	39.1 ± 13.1	16.8 ± 1
	25%	63.4 ± 21.8	27.3 ± 1.6
	50%	110.4 ± 38.7	53.5 ± 1.9
	100%	233.7 ± 86	-

Table 2: Summary of motor unit physiology in male participants in adduction 60, internal rotation, adduction 90, flexion, and horizontal adduction at 15% and 25% MVF. 50% MVF is also reported for horizontal adduction. The number of motor units, including the number of participants, successfully decomposed, is included in column 3. Mean discharge rate and CoV inter-spike interval with standard deviation for each task and force level is also reported. Statistical analyses between 15% and 25% MVF within a task for EMG amplitude, discharge rate, and coefficient of variation are reported in columns 7 through 9. Bolded numbers denote significant differences between force levels within a task. DR: discharge rate; CoV: coefficient of variation.

Task	Force level (%MVF)	Number of motor units (Number of participants)	Mean EMG amplitude (%MVF)	Statistical comparisons (EMG amplitude)	Mean DR across sustained hold (pps)	Statistical comparisons (DR)	Coefficient of Variation	Statistical comparisons (CoV)	Mean DR in the first 5 seconds of the sustained hold (pps)
Adduction 60	15	13 (N = 8)	8.5 ± 3.3	**t_7 = -4.07, p = 0.004, *d* = 1.42**	13.8 ± 2.4	t_7 = -0.65, p = 0.53	15.9 ± 2.7	t_7 = -2.16, p = 0.06	14.2 ± 2.6
	25	13 (N = 8)	13.3 ± 5		14.4 ± 1.4		19.1 ± 4		15.2 ± 2.2
Internal rotation 60	15	16 (N = 6)	9.1 ± 6.4	**t_5 = -4.38, p = 0.007**	13.9 ± 1.1	t_5 = -0.83, p = 0.44	18.2 ± 3.4	t_5 = -1.23, p = 0.27	14.6 ± 0.4
	25	16 (N = 6)	13 ± 4.9		14.5 ± 1		19.1 ± 2.4		15 ± 1.7
Adduction 90	15	16 (N = 7)	6.5 ± 3.9	**t_6 = -4.24, p = 0.005, *d* = 1.58**	12 ± 3.6	t_6 = -0.38, p = 0.71	21.1 ± 5.7	t_6 = 0.50, p = 0.63	12.7 ± 4
	25	16 (N = 7)	10.8 ± 3.8		12.3 ± 3.4		19.7 ± 5.7		12.9 ± 3.2
Flexion	15	13 (N = 5)	11.7 ± 6.5	**t_4 = -7.66, p = 0.001, *d* = 3.14**	13.2 ± 1.6	t_4 = -0.92, p = 0.41	18.5 ± 4	t_4 = -0.41, p = 0.69	14.6 ± 2.1
	25	13 (N = 5)	16.1 ± 5.5		13.9 ± 1.6		19.4 ± 4.2		16.4 ± 1.7
Horizontal adduction	15	19 (N = 6)	9.2 ± 3.3	**t_4 = -5.42, p = 0.005**	14.6 ± 2.5	t_5 = 2.44; p = 0.058	15.9 ± 3.1	t_5 = -2.58, p = 0.049	17.5 ± 3.2
	25	19 (N = 6)	14.3 ± 4.5		12.9 ± 2.4		21.8 ± 5.7		16.1 ± 3.1
Horizontal adduction	25	23 (N = 4)	12.3 ± 4.9		13.7 ± 2.7	t_3 = -2.20, p = 0.11	16.7 ± 4.4	t_3 = -2.02, p = 0.13	16.1 ± 1.6
	50	23 (N = 4)	27.7 ± 10.8		15.9 ± 2.8		19.7 ± 2.2		18.7 ± 3.6

Table 3: Summary of motor unit physiology in *female* participants in adduction 90, internal rotation, and adduction external 90 tasks at 15% and 25% MVF. The number of motor units, including the number of participants, successfully decomposed is included in column 3. Mean discharge rate, Coefficient of Variation (with standard deviation) for each task, and force level is also reported.

Task	Force Level (%MVF)	Number of Motor Units (Number of Participants)	Discharge Rate (pps)	Coefficient of Variation
Adduction 90	15	18 (N = 5)	9.4 ± 1.3	17.3 ± 2.1
	25	4 (N = 3)	9 ± 2.1	19.7 ± 4.1
Internal Rotation 60	15	5 (N = 2)	14.8 ± 1.2	14.1 ± 0.8
	25	1 (N = 1)	12.1	15.9
Adduction External 90	15	10 (N = 2)	8.8 ± 0.6	17.9 ± 0.5
	25	9 (N = 3)	9.9 ± 0.6	17 ± 1.5

Neural control of the healthy pectoralis major from low-to-moderate isometric contractios